Magnetic switching of Fe-porphyrin molecules adsorbed on surfaces: An XAFS and XMCD study

Journal of Physics: Conference Series **190** (2009) 012012 doi:10.1088/1742-6596/190/1/012012

Magnetic switching of Fe-porphyrin molecules adsorbed on surfaces: An XAFS and XMCD study.

Klaus Baberschke†

Institut für Experimentalphysik, Freie Universität Berlin, Arnimallee 14, D-14195 Berlin, Germany

Abstract. Metalorganic molecules like Fe-porphyrin or haemoglobin have been investigated in great detail in the past. Its importance is obvious and has been measured mostly with molecules in random orientation. Here we report on experiments of a single monolayer of Fe-porphyrin in UHV aligned flat on ferromagnetic Ni and Co films. NEXAFS with linear and circular polarization is the spectroscopy of choice; it is elementspecific and measures the electronic structure as well as the magnetism at once. For the flat oriented monolayer of porphyrin molecules we have measured the angular dependence of XAFS at the C and N K-edge and XMCD at the Fe L-edges. The paramagnetic Fe-spin is aligned with respect to the ferromagnetic substrate. This can be parallel or antiparallel. Also nonmagnetic substrates like Cu (100) plus an external magnetic field will align the magnetic Fe-moment. This altogether opens a huge field for switching the 3d-spin from parallel to perpendicular of the molecular plane, which in turn will modify the electronic transport properties and act as a *single molecular switch*.

PACS numbers: 75.70.-i,78.70Dm

1. Introduction

Metalorganic molecules like porphyrin, phthalocyanine, or chlorophyll are highly important. A metal ion (Fe, Co, Zn, Mg) is surrounded by an alternating nitrogen-carbon-ring of pyrrole structure and/or C-H substituents endings. X-ray absorption fine structure spectroscopy (XAFS) is the technique of choice to investigate these molecules, because it is elementspecific and can probe the metal, and the ligand (N and C) ions at the same time. The K-edges of N and C, as well as the L-edges of Fe, Co are in the same energy range (200 - 900 eV) of the soft X-ray regime. Using linear polarization, NEXAFS detects above and below threshold the giant scattering profiles of the photoelectron (σ^*-shape resonances) and transitions into unoccupied bound states (π^*, LUMO). If the molecules are oriented flat on a single crystal surface, the angular dependence of NEXAFS gives very useful information about the orientation and the geometrical structure - see the early work on simple diatomic molecules [1] and as a case study the simple organic acetonitrile with two different ions (C,N)[2]. In addition, circular polarization of the synchrotron radiation can be used to measure the X-ray magnetic circular dichroism (XMCD). The magnetic moment of the center 3d-metal ion may be aligned by an external magnetic field H or an internal exchange coupling $H_{\rm exch}$. With this, a manipulation of the molecular magnetism becomes

† E-mail: bab@physik.fu-berlin.de

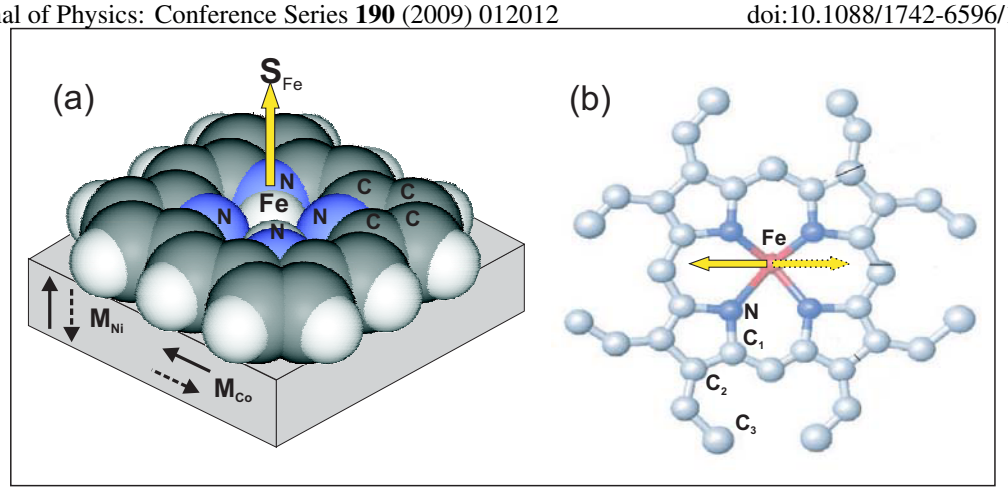

Figure 1. In Fig.1a the schematic molecule on an ultrathin ferromagnetic Ni or Co film is shown in a space filling model. The central metal ion is surrounded by 4 pyrrole rings with nitrogen as nearest neighbors. This part of the molecule has almost planar structure. At the outer peripherie additional substituents are bonded, e.g. tetraphenyl (TPP), or octaethyl (OEP, as shown in Fig.1b). These parts are oriented out-of-plane.

possible and that, in turn, will also change the electric transport properties. On todays level, to measure this magnetism by XMCD is highly important because these molecules may serve as molecular switches in nanoelectronics.

Numerous work has been published for XAFS in bulk metalorganic materials, we cite only few: The standard review by Penner-Hahn and Hodgson for the XAS of iron porphyrin [3] in the soft X-ray regime. Recently the Stanford-Utrecht group has measured and calculated in great detail the delocalization of Fe d-electrons in porphyrin like molecules by means of XAS at the L-edges of Fe [4]. Goulon et al. have given a comprehensive overview for porphyrin XAS in experiment and theory for the hard X-ray regime (2000 - 8000 eV) [5]. Both [3, 5] include also the extended energy range (EXAFS). Most of these experiments work with powder, or unoriented molecules. Consequently in the spectra the angular dependent information is missing, be it for the π^*-transition or the σ^*-shape resonances. Todays high sensitivity of the 3rd generation synchrotron facilities and the advanced UHV surface science technique allow the preparation and XAS experiments for molecular monolayers (ML) on atomically flat single crystal surfaces [6, 7, 8, 9], see also STM and PE work [10, 11, 12].

Here we will focus on an iron-porphyrin monolayer to demonstrate the capability of XAFS and XMCD. Fig.1a shows the almost planar central part of the molecule, a metal ion with 4 pyrrole rings. In Fig.1b the full molecule with 8 ethyl substituents is sketched. Our experiments [13, 14, 15] focus on this octaethylporphyrin (OEP), but others with tetraphenylporphyrin (TPP) have been published as well. The molecules are evaporated in UHV and adsorb flat on a metal single crystal surface. 1 ML of OEP flat on a non magnetic surface of Cu(001), for example, corresponds approximately to 1/100 ML of Fe/Cu(001). The lateral distance of the Fe magnetic moments will be $\approx$ 10Å; at finite temperature it will be a paramagnetic (disordered) state. Direct Fe-Fe dipolar coupling will be very weak, in the order of 1 K. If ,however,

the substrate crystal is a ferromagnet the exchange coupling can be very large (10 - 100 meV), and the iron magnetic moments μ_{Fe} are aligned with respect to the magnetization of the ferromagnet, in-plane for an ultrathin Co film and out-of-plane for $\approx$ 15 ML Ni/Cu(001) [13]. In addition the coupling can be manipulated to be ferro- or antiferromagnetic depending on the exchange constant being positive or negative [15]. In a similar way an external magnetic field can be used to *switch* Fe-spins in a given direction [8]. This will be discussed in Sec.3. Firstly, in Sec.2, we verify the geometry and orientation of the molecules by means of the angular dependent K-edge NEXAFS. This full set of information (K- and L-edges, linear and circular polarization) is missing in many of the other published results, although it contains relevant information.

2. NEXAFS at the C and N K-edges

The X-ray absorption spectrum at the K-edges of C and N in metalorganic molecules have two distinguished different parts [16]: (i) Below threshold there are transitions of the $1s$ electron into an unoccupied bound state (π^*, LUMO, Rydberg, etc.). This is a discrete transition and a relaxation back to the groundstate. The narrow lines are easy to detect and are analyzed mostly with symmetric (Lorentz-, Voigt-) profiles - however, in principle, they are asymmetric due to the vibrational fine structure [17]. (ii) Above threshold the 1s photoelectron escapes into the continuum. The core electron is trapped temporarily by a centrifugal barrier [18]. This approach is known as the multiple scattering model. The physical ideas underlying refer to a simple quantum mechanical scattering model, the exited $1s$ photoelectron escapes to a continuum of final states. Near to threshold these are quasibound states of the inner well potential. For small energies above threshold (10 - 30eV) the detailed shape of the potential is less important (Schwinger's theorem 1947), a spherical well potential of depth V_0 and

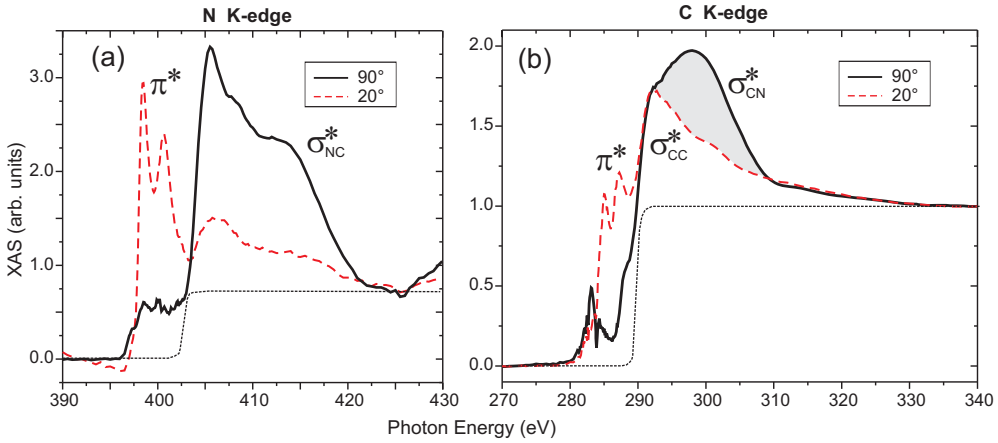

Figure 2. NEXAFS spectra at N and C K-edge for normal and grazing incidence, taken at $T = 300K$ [13]. Below threshold the π^*-transitions are indicated and discussed in [13, 15]. Above threshold the scattering profile for the shape resonances are seen. At the C edge only a part (gray area) is angular dependent and is attributed to the C-N and C-C bond axis, oriented parallel to the surface [20].

radius a is a good assumption ([18, 19] and references therein). Such a simple model potential has the advantage of an analytical solution yielding the full line shape of the resonance signal. These so called σ^*-shape resonances have an asymmetric profile with high energy tail [19].

In Fig.2 the NEXAFS spectra are shown for Fe-porphyrin on a ultrathin film Ni/Cu(001)[13]. For normal incidence strong intensities in the regime of the σ^*-shape resonances are measured. For grazing incidence they disappear (almost) completely at the N edge, whereas at the C edge only a part vanishes (gray area). This can be understood easily from Fig.1. N is bonded to Fe and 2 C_1-ions, all in plane. In contrast, for the carbon there are different ions some with the bond axis in-plane, others with bonding out-of-plane ($C_2 - C_3$), for which the shape resonances in average are angular independent - like in powder. The corresponding angular dependence of the π^*-transitions support this picture. So, we attribute the angular dependent σ^*-shape resonance at approx. 300 eV to the N-C bonding and its molecular potential. In Fig.3a and b the difference spectra ($90^0 - 20^0$) display better the shape of the resonance profile. This is shown by the simulation (red dashed line) in Fig.3 (taken from [20], details will be published elsewhere). In addition Fig.3c show the same profile of the shape resonance in the original XAS spectrum at the N K-edge. To fit such an asymmetric scattering profile (red dashed line in Fig. 3a-c) is less popular in nowadays, but instructive. For details we refer to [19] and its application in [18, 17]. To conclude, such a scattering at a spherical well potential of the N-C bonding must explain the scattering from both sides ($N \Leftrightarrow C$). σ^*- shape resonances give direct access to the geometry, i. e. the scattering of the photoelectron at the n.n. potential. The angular sensitivity of the E1 transition probability probes the direction to the n. n. Whereas the angular dependent transition probability to unoccupied final states, measure energy differences and in an indirect way the geometry. The present NEXAFS results at C- and N-edges confirm the flat lying porphyrin molecules on the surface [21].

Beside the angular dependence and its quantitative line shape analysis, other information can be measured at the N, C edges. In [4, 6] and others the charge transfer and bonding is discussed. But it is also known, that polarized spin transfer

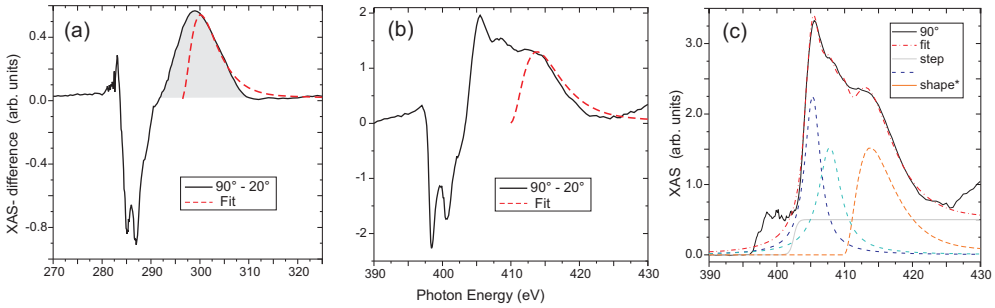

Figure 3. In Fig.3a the difference ($90^0 - 20^0$)spectrum is plotted. The gray area fits to a scattering profile with strength of $V_0 a^2 = 7.3$ eVÅ^2 [20, 18]. In Fig.3b the same fit is shown for the spectrum at the N edge, it fits the high energy tail satisfactory. Close to the edge additional - non C-N scattering - appears. To visualize the shape resonance profile better at the N ion, in Fig.3c the same fit (red dashed) is plotted in the original NEXAFS.

happens [22]. This was measured by means of ESR as transfered hyperfine interaction. In principle, XMCD at the K-edges should detect this also. Unfortunately the orbital magnetic moment is detectable, only, which will be very small. One example for oxygen is given in [23]. At the N K-edge of the Fe-porphyrin no XMCD signal was detected, yet.

3. NEXAFS and XMCD at the Fe $L_{3,2}$-edges

3.1. $3d^n$-energy scheme and magnetism of the Fe-ion

Fe-ions in porphyrin and similar metalorganic molecules have a huge variety of different electronic and magnetic ground states. Iron may be ferric $3d^5Fe^{3+}$ with half-integer spin of $S = 5/2, 3/2, 1/2$. Or it can be ferrous $3d^6Fe^{2+}$ with integer spin of $S = 2, 1, 0$. Which of these configurations (high- or low-spin) will be the ground state is determined by ligand- (crystal-) field splitting (CEF, Fig.4). For a single layer of molecules this is very sensitive to the local adsorption geometry, additional gaze dosage, etc. Clearly we have no cubic (O_h) symmetry, axial symmetry with the z-axis normal to the molecular plane (D_{4v}) is more realistic. The question arises, is the cubic CEF larger or smaller than the low symmetry contribution - as indicated in Fig.4a and Fig.4b, respectively? This influences high or low spin being the ground state. For bulk crystals Fig.4a will be the standard case (Hund's rules). But for a monolayer this may depend very much on the hybridization to the substrate and on additional adsorption of other molecules, oxygen for example. This has been shown for Fe-terephthalate acid (Fe-TPA) [7] and for Fe-porphyrin [15]. In [7] the initial splitting (Fig.4a) switches to Fig.4b after oxygen adsorption.

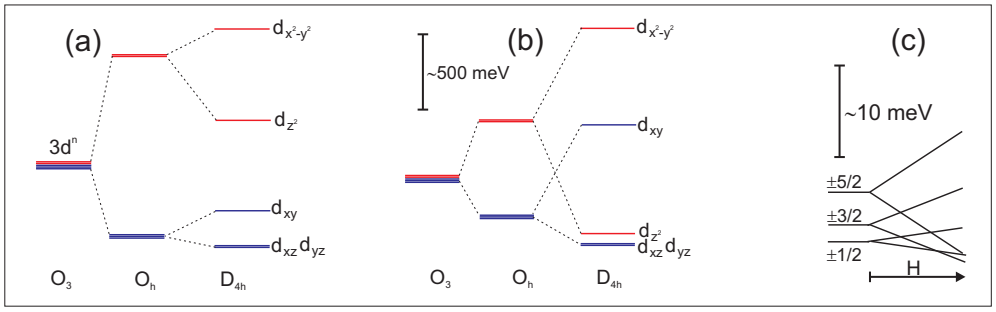

Figure 4. Schematic energy scheme for the d-states. Fig.4a and 4b show the crystal field splitting (CEF) for the cubic O_h contribution being larger(a)/smaller(b) than the tetragonal D_{4v} contribution. In Fig.4c the zero field splitting and the Zeeman term is added, assuming an S=5/2 ground state. The diagram is indicative and not to scale, note the different scales for a,b and c. See text.

We would like to point out, that the commonly used notation of the unperturbed $3d$ orbitals ($d_{z^2}, d_{x^2-y^2}, d_{xy}, d_{xz}, d_{yz}$) serve as a label , but may be misleading using it for a physical interpretation, because the real orbitals, eigenstates are quite different. The spin-orbit coupling λ**LS** mixes the unperturbed O_h eigenstates. One might say, that λ**LS** is a small perturbation. Yes, but it is the only and important source for magnetic anisotropy, that is to say, it creates the anisotropic magnetic moment, the g-tensor. The ratio of the ligand field parameters and the spin-orbit coupling Δ/λ is the

controlling parameter for mixing of e_g and t_{2g} states. For example, the diagonal term $\lambda L_z S_z$ mixes $d_{x^2-y^2}$ and d_{xy}. The off-diagonal $\lambda L_{\pm} S_{\mp}$ mixes d_{xy} with d_{xz}, d_{yz} and shifts the corresponding spin eigenstates. This is the origin of magnetic anisotropy in a paramagnetic molecule. It is a well established technique in EPR to measure the g-tensor components and deduce from this the low- or high-spin states and the strong or weak ligand field parameters [24, 25]. We refer to [22], the authors measured several paramagnetic cofactor heme systems and deduced a low-spin ferric porphyrin. They also discuss the magnetic coupling between Fe and the N-nucleus. In analogy, XMCD should be able to detect an induced magnetic moment at the nitrogen n.n. In conclusion, the e_g and t_{2g} terminology, frequently used in PES, is correct only for perfect cubic symmetry; it can never explain hysteresis and coercive fields in paramagnetic Fe molecules - like in [8] and in Fig.5c,d. The expectation value of the orbital moment will always remain zero ($< L_z >= 0$) for the unperturbed d-orbitals ($d_{z^2}, d_{x^2-y^2}, d_{xy}, d_{xz}, d_{yz}$). For surface and molecular physics one needs to go beyond that to explain magnetic anisotropy, spin transfer, orbital polarization, etc. For spin multiplicity of $S > 1/2$ spin-orbit coupling and the low symmetry CEF splits the $(2S+1)$ degeneracy in Kramer doublets, the so called *zero field splitting*, as indicated in Fig.4c; for iron heme system typical in the range of ≈1 meV.

In the present work we would like to switch the paramagnetic Fe-spin by means of a magnetic field (H, H_{exch}). Applying a magnetic field, the Zeeman term needs to be added in the energy scheme, as sketched in Fig.4c. The Zeeman splitting will be smaller than the CEF, but it is large enough to cross or mix the eigenstates. For H or H_{exch} $\perp$ to the molecular plane (Ni in Fig.1a) the Zeeman term and CEF will be diagonal, resulting in level crossing (Fig.4c). For H $\parallel$ to the molecular plane (with Co-substrate in Fig.1b and 5b) both parts of the Hamiltonian are non-diagonal and produce level repulsion and non-linear magnetic field dependence.

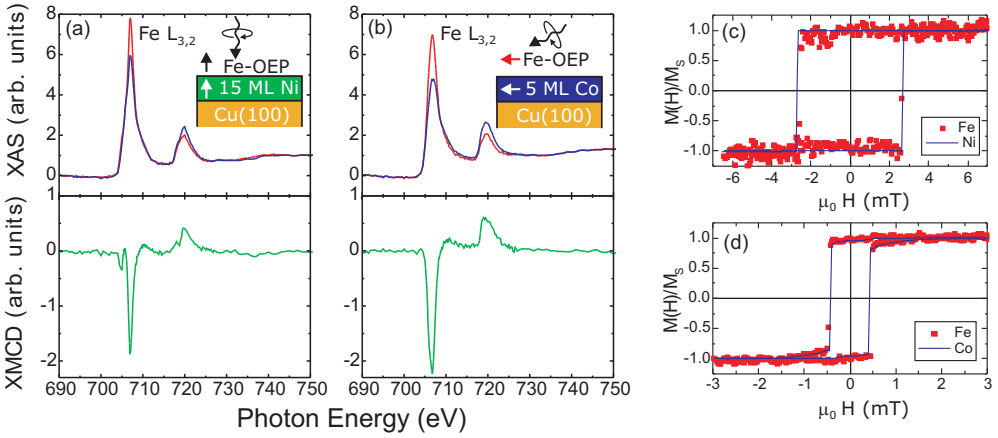

Figure 5. Fe L-edge XAS and XMCD spectra of a monolayer of Fe-OEP on ultrathin ferromagnets of Ni (Fig.5a) and Co (Fig.5b) taken at $T = 300K$ [13, 14]. The corresponding square like hysteresis loops taken at the XMCD maximum of the L_3 edges are displayed in Fig.5c,d. Note that the external field points not along the easy axis of the Co film, resulting in a smaller coercive field.

3.2. L-edge spectra

For 15 ML Ni/Cu(100) the easy axis of magnetization is pointing $\perp$ to the surface [26], parallel to the symmetry z-axis of the porphyrin . In Fig.5a the XAS and XMCD spectra at the Fe $L_{3,2}$ edge are shown for normal incidence. A strong Fe-XMCD is detected, indicating that all Fe moments are aligned parallel to the surface normal. The negative signal at L_3 is defined as M_{Ni} been $\parallel$ to the moment of Fe OEP, i.e. μ_{Fe} is ferromagnetic coupled. The exchange coupling was determined to be in the range of 50 meV. (For details and temperature dependence see [13, 14]). If we apply in addition a small external field of few mT, it is very easy to flip M_{Ni} up and down. This hysteresis loop is shown in Fig.5c, the Fe moment μ_{Fe} (red data points) follows [28] exactly in a square like loop. We would predict that in a STM experiment, which measures the electric transport perpendicular to the plane, different conductance will be recorded (see Sec.3.1). For Co-phthalocyanine molecules on Co/Cu(111) this has been observed recently in [27].

For molecular electric circuits the conductivity in-plane is of equal importance [28]. Few layers of Co/Cu(100) with easy axis in-plane, simulate this situation. In Fig.5b the corresponding spectra with grazing incidence are displayed. Again the Fe moment and M_{Co} are ferromagnetically coupled. Similar elementspecific hysteresis loops are observed (Fig.5d). Only few mT are needed to flip M_{Co} and the Fe-spin at 300K. The first experiments of this kind have been performed by Scheybal et al. [29] on Mn porphyrin. One monolayer of Mn-TPP was evaporated on a thick Co/Au substrate. Elementspecific hysteresis loops in-plane (like Fig.5d) were recorded, with the Mn spin "switching" in-plane from plus to minus.

The application of the *sum rules* in XMCD allows also to determine the orbital and spin moments, μ_{orb}, μ_S. This has been discussed for Fe-OEP in [13] and for Mn in [8]. We would like to mention, that this is accompanied with difficulties: (i) Due to the T_z-term only an "effective" spin moment can be tabulated. More reliable is to determine the ratio μ_{orb}/μ_S, only. For our system we measured a ratio of 5 - 10% [14]. (ii) In particular for Mn and other "early" 3d-elements, the application of the *sum rules* is questionable [30]. Electron spin resonance, like in [22] seems to be a "safer" technique to determine the true spin- and orbital moments (see Sec.3.1)

The results in [29, 13, 14] show clearly that the exchange coupling of the 3d-metalorganic molecules with the ferromagnetic Co or Ni films is very strong; already at 300 K saturation (complete alignment) of the paramagnetic Fe/Mn-porphyrin is reached. It may be of technological interest also, to switch the molecular magnet by an external field, without a ferromagnet. Mannini *et al* reported XAS/XMCD experiments on Fe_4-metalorganic molecules. They used $H = \pm 1.5T$ and very low temperatures of $T = 0.5K$ [8]. Under these conditions they reached almost complete saturation and hysteresis loops of the Fe_4-complexes. For our Fe-OEP current experiments are under investigation. With $H = \pm 5T$ and $T = 7K$ only a small percentage of alignment (Brillouin function) was reached.

In Sec.3.1 we discussed the high sensitivity and balance of the ligand field parameters and the spin-orbit coupling. Intuitively it is clear, that small modifications of the organic molecules (OEP $\Leftrightarrow$ TPP, hybridization with substrate, adsorption of additional molecules, etc.) will change this balance. In [7] a self-assembly supra-molecular $Fe(TPA)_4$ complex was investigated without and with additional O_2 dosage. For O_2-Fe(TPA)$_4$ the cubic CEF is larger than the tetragonal CEF (like Fig.4a) and for $Fe(TPA)_4$ without O_2 it's the other way around (Fig.4b). For the

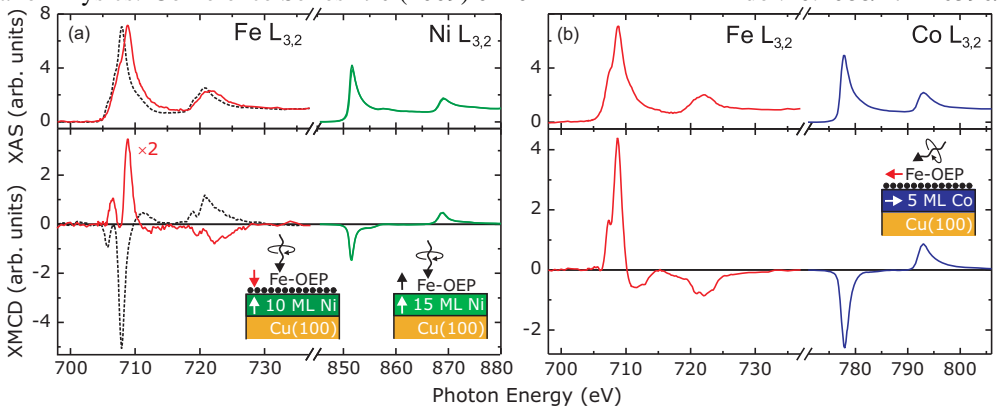

Figure 6. Same as in Fig.5a and b, however with 1/2 ML c(2x2) of oxygen (black dots in the inset) on top and measured at 40 K [15]. For details see [23, 15] and references therein. In Fig.6a on the right hand side spectra without oxygen are plotted for comparison. The arrows in the inset indicate antiferromagnetic coupling between Fe and the ferromagnet after oxygen treatment.

Fe-OEP monolayer we have performed a similar experiment: It is known that half a monolayer of O/Cu(100) acts as a surfactant for the growth of Ni or Co films on Cu(100). As a result the oxygen with a c(2x2) structure will float on top of Ni/Cu(100), Co/Cu(100) films, respectively [23]. What will happen with a porphyrin monolayer evaporated on top of this, will the direct exchange be reduced, is there new superexchange? In contrast to Fig.5 where the iron moments points always parallel to the substrate magnetization, we see in Fig.6a and b that for the oxygen ligated Fe-porphyrin the Fe XMCD signal has opposite sign with respect to the substrate magnetization [15]. This is indicated with antiparallel arrows in both insets of Fig.6. For comparison Fig.6a displays also spectra of Fe-OEP on Ni/Cu(100) without oxygen, confirming the ferromagnetic coupling. In principle it is not that surprising, that via the $2p$ orbitals of oxygen an antiferromagnetic superexchange acts. However, for the molecular nanomagnetism it opens a huge field of new manipulation.

The XAS spectra in Fig.6a show a shift of the L_3 line to higher energies for the oxygen ligated case, this is attributed to a divalent Fe state without oxygen and a trivalent state with oxygen coverage. As discussed before, the determination of the spin state is not so easy in this experiment. Only the T-dependence of the magnetization (Fig.2 in Ref.[15]) gives some indication. For both experiments an intermediate spin state of S=1 and 3/2, respectively, is likely. In other words, very likely the Fe groundstate is: ferrous $3d^6 Fe^{2+}$ with $S = 1$ for the metallic substrate and ferric $3d^5 Fe^{3+}$ with $S = 3/2$ for the oxygen surfactant grown film [15].

4. Discussion, Summary

The key message of the present work is, that the combination of elementspecific XAFS with todays UHV surface physics of oriented molecular monolayers opens the full capability of angular dependent XAFS and XMCD. If, in addition, external or internal magnetic fields align the magnetic moment of the paramagnetic Fe-OEP, or for example in hemoglobin, additional information can be gained about the magnetic

groundstate. In the future it may be realistic to produce and analyze *single molecular magnetic switches*. The characteristic features required for the application are twofold: (i) A moderate exchange coupling between FM film and the Fe-OEP is required to flip all Fe-spins. The given values for Fe-OEP on Ni- or Co-films [13, 15] are sufficient. Flipping by an external field only, without FM film [8] seems to be less applicable. (ii) For technological application only small external fields are desired for easy switching. That depends on the coercive field of the FM ultrathin film. This can be manipulated by temperature and by the growth modus of the ultrathin film. In [9] the recent progress in "magnetic molecules on surfaces" has been discussed. It looks very promising not only for "new spintronic applications" but also for fundamental understanding. Full experimental evidence is needed in the future about the real adsorption geometries. Is the Fe-ion of Fe-OEP absorbed exact on top of the c(2x2) O on Ni/Cu(100) [15], confirming the classical superexchange? What is the exact position of the pyrrole N-ions, does it support the 90^0-exchange between the Ni/Co ferromagnet and the Fe-porphyrin [13] ? The extended energy range of the X-ray absorption fine structure (EXAFS) will be a good tool to answer these questions and give a better input for electronic-structure calculation to study ligand-to-metal donation, back bonding, and valence delocalization.

Finally, we would like to mention that the use of synchrotron radiation and electron paramagnetic resonance, EPR, are merging together. In early days both communities were running quite different and separate routes. At BESSY II Schnegg et al. [31] used the storage ring in the low α mode as a frequency generator. The radiation ranges from 150 GHz to 1.2 THz. This radiation was used for an EPR experiment at the prototype of a single molecular magnet, the Mn_{12}Ac with a total spin of $S = 10$. This molecule has a large zero field splitting - see Fig.4c. At low temperatures and depending on the external magnetic field, the authors observe indeed $\Delta M = \pm 1$ spin transitions in the frequency range of 300 GHz. In the future synchrotron radiation may be used for THz-EPR.

Acknowledgment

The present work has been performed mainly in collaboration with H. Wende and with the other co-authors of ref [13, 14, 15]. E. Kosubek and J. Kurde are acknowledged for assistance in preparing this manuscript. The work was initiated and supported by grants: BMBF 05KS4-KEB (Wende/Baberschke), Sfb 658, and Sfb 491.

References

[1] Stöhr J, Baberschke K, Jaeger R, Treichler R, Brennan S 1981 Phys. Rev. Lett. **47** 1301
[2] Neumann A, Rabus H, Arvanitis D, Solomun T, Christmann K, Baberschke K 1993 Chem. Phys. Lett. **201** 108
[3] Penner-Hahn J E and Hodgson K O, in *Iron Porphyrins* Part **3**, Lever A B P, Gray H B, Eds. (J. Wiley and Sons, New York-London, 1989)
[4] Hocking R K, Wasinger E C, Yan Y L, de Groot F M F, Walker F A, Hodgson K O, Hedman B, Solomon E I 2007 J. Am. Chem. Soc. Vol.**129** 114
[5] Goulon J, Goulon-Ginet Ch, and Gotte V, in *The Porphyrin Handbook* Vol.**7**, Kadish K M, Smith K M, Guilard R, Eds. (Academic Press, New York, 2000)
[6] Narioka S, Ishii H, Ouchi Y, Yokoyama T, Ohta T, Seki K 1995 J. Phys. Chem. **99** 1332
[7] Gambardella P, Stepanow S, Dmitriev A, *et al*, 2009 Nature Materials **8** 189
[8] Mannini M, Pineider F, Saintavit P, *et al*, 2009 Nature Materials **8** 194
[9] Wende H 2009 Nature Materials **8** 165
[10] Barth J V, Costantini G, and Kern K, Nature **437**, 671 (2005)

[11] Grill L, Dyer M, Lafferentz L, Persson M, Peters M V, Hecht S 2007 Nature Nanotech. **2** 687
[12] Gottfried J M, Flechtner K, Kretschmann A, Lukasczyk T, and Steinrück H-P, J. Am. Chem. Soc. **128** 5644-5645 (2006).
[13] Wende H, Bernien M, Luo J, Sorg C, Ponpandian N, Kurde J, Miguel J, Piantek M, Xu X, Eckhold Ph, Kuch W, Baberschke K, Panchmatia P M, Sanyal B, Oppeneer P M, Eriksson O 2007 Nature Materials **6** 516
[14] Bernien M, Xu X, Miguel J, Piantek M, Eckhold Ph, Luo J, Kurde J, Kuch W, Baberschke K, Wende H, Srivastava P 2007 Phys. Rev. B **76** 214406
[15] Bernien M, Miguel J, Weis C, Ali M E, Kurde J, Krumme B, Panchmatia P M, Sanyal B, Piantek M, Srivastava P, Baberschke K, Oppeneer P M, Eriksson O, Kuch W, Wende H 2009 Phys. Rev. Lett. **102** 047202
[16] Nenner I, in *Giant Resonances in Atoms, Molecules and Solids* NATO ASI Series Vol. **151** p. 259 Connerade J P, Estava J M, Karnatak R C, Eds. (Plenum Press, New York-London, 1987)
[17] Rabus H, Arvanitis D, Domke M, Baberschke K 1992 J. Chem. Phys. **96** 1560
[18] Arvanitis D, Rabus H, Wenzel L, Baberschke K 1989 Z. Phys. D **11** 219
[19] Connerade J P in *Giant Resonances in Atoms, Molecules and Solids* NATO ASI Series Vol. **151** p. 3 Connerade J P, Estava J M, Karnatak R C, Eds. (Plenum Press, New York-London, 1987)
[20] Bovenschen D, Diplom Thesis 2009 University Duisburg-Essen, unpublished
[21] When analyzing the profile of σ^*-shape resonances the equation of chapter 7.2.3 in the textbook *NEXAFS Spectroscopy* by J. Stöhr (Springer Series in Surface Sciences **25**) is used commonly. We would like to point out, that these equations include a typographical error leading to an erroneous line shape. We refer to the correct one in [19, 18].
[22] Fahrenschmidt M, Bittl R, Rau H K, Haehnel W, Lubitz W 2000 Chem. Phys. Lett. **323** 329
[23] Sorg C, Ponpandian N, Bernien M, Baberschke K, Wende H, and Wu R Q, 2006 Phys. Rev. B **73** 064409
[24] Abragam A, Bleaney B *Electron Paramagnetic Resonance of Transition Ions* Marshall W, Wilkinson D. H, Eds. (Clarendon Press, Oxford, 1970), see also Part **2** of [3]
[25] K. Baberschke in *Handbook of Magnetism and Advanced Magnetic Materials*, Volume **3**, p.1617 Edited by Helmut Kronmüller and Stuart Parkin, 2007 John Wiley & Sons
[26] Schulz B, Baberschke K 1994 Phys. Rev. B **50** 13467
[27] Iacovita C, Rastei M V, Heinrich B W, Brumme T, Kortus J, Limot L, Bucher J P, 2008 Phys. Rev. Lett. **101** 116602
[28] Kiguchi M, Tal O, Wohlthat S, Pauly F, Krieger M et al. 2008 Phys. Rev. Lett. **101** 046801
[29] Scheybal A, Ramsvik T, Bertschinger R, Putero M, Nolting F, and Jung T A, Chem. Phys. Lett. **411**, 214 (2005).
[30] Scherz A, Gross E K U, Appel H, Sorg C, Baberschke K, Wende H, Burke K 2005 Phys. Rev. Lett. **95** 253006
[31] Schnegg A, Behrends J, Lips K, Bittl R, Holldack K 2009 Phys. Chem. Chem. Phys. online 23rd June